

# Graph Kolmogorov–Arnold Networks for Multi-Cancer Classification and Biomarker Identification: An Interpretable Multi-Omics Approach

Fadi Alharbi<sup>1,2</sup>, Nishant Budhiraja<sup>1</sup>, Aleksandar Vakanski<sup>1</sup>, Boyu Zhang<sup>1</sup>, Murtada K. Elbashir<sup>3,4</sup>, and Mohanad Mohammed<sup>5</sup>

<sup>1</sup>College of Engineering, Department of Computer Science, University of Idaho, Moscow, ID 83844, USA; alha5622@vandals.uidaho.edu, budh1430@vandals.uidaho.edu, vakanski@uidaho.edu, boyuz@uidaho.edu

<sup>2</sup>College of Computer and Information Sciences, Department of Computer Science, Jouf University, Sakaka, Aljouf 72441, Saudi Arabia; faalharbi@ju.edu.sa

<sup>3</sup>College of Computer and Information Sciences, Department of Information Systems, Jouf University, Sakaka, Aljouf 72441, Saudi Arabia; mkelfaki@ju.edu.sa

<sup>4</sup>Faculty of Mathematical and Computer Sciences, University of Gezira, Wad Madani, Sudan; murtadabashir@uofg.edu.sd

<sup>5</sup>School of Mathematics, Statistics and Computer Science, University of KwaZulu-Natal, Pietermaritzburg, Scottsville, 3209, South Africa; mohanadadam32@gmail.com

Corresponding author: Aleksandar Vakanski (vakanski@uidaho.edu).

## Abstract

The integration of multi-omics data presents a major challenge in precision medicine, requiring advanced computational methods for accurate disease classification and biological interpretation. This study introduces the Multi-Omics Graph Kolmogorov–Arnold Network (MOGKAN), a deep learning model that integrates messenger-RNA, micro-RNA sequences, and DNA methylation data with Protein-Protein Interaction (PPI) networks for accurate and interpretable cancer classification across 31 cancer types. MOGKAN employs a hybrid approach combining differential expression with DESeq2, Linear Models for Microarray (LIMMA), and Least Absolute Shrinkage and Selection Operator (LASSO) regression to reduce multi-omics data dimensionality while preserving relevant biological features. The model architecture is based on the Kolmogorov–Arnold theorem principle, using trainable univariate functions to enhance interpretability and feature analysis. MOGKAN achieves classification accuracy of 96.28% and demonstrates low experimental variability with a standard deviation that is reduced by 1.58–7.30% points compared to Convolutional Neural Networks (CNNs) and Graph Neural Networks (GNNs). The biomarkers identified by MOGKAN have been validated as cancer-related markers through Gene Ontology (GO) and Kyoto Encyclopedia of Genes and Genomes (KEGG) enrichment analysis. The proposed model presents an ability to uncover molecular oncogenesis mechanisms by detecting phosphoinositide-binding substances and regulating sphingolipid cellular processes. By integrating multi-omics data with graph-based deep learning, our proposed approach demonstrates superior predictive performance and interpretability that has the potential to enhance the translation of complex multi-omics data into clinically actionable cancer diagnostics.

**Keywords:** Cancer classification, gene expression analysis, multi-omics data integration, graph attention networks, Kolmogorov–Arnold Networks, protein-protein interaction networks.

## 1. Introduction

Cancer is a highly heterogeneous disease driven by genetic, epigenetic, and transcriptomic alterations in cells. Recent advances in high-throughput sequencing have enabled the generation of multi-omics datasets, providing deeper insights into the factors influencing cancer development and patient outcomes. However,

extracting meaningful insights from datasets faces significant challenges due to their high dimensionality, feature heterogeneity, and complex genomic structures [1], [2]. While traditional machine learning methods, such as Support Vector Machines (SVMs) and Random Forests (RF), have shown promise in multi-omics cancer classification, they often struggle with modeling high-dimensional data and feature interpretability [3], [4].

Graph Neural Networks (GNNs) have demonstrated strong capability in capturing complex biological network relationships. Unlike models employing Euclidean-based data representations, GNNs leverage a graph-based structure to efficiently represent interactions among genes, proteins, and regulatory elements [5], [6]. Graph Attention Networks (GATs) stand out as a superior GNN variant for biomedical applications as they dynamically assess node importance [7]. While GNNs achieve high classification performance, their limited interpretability hinders biomarker discovery and the understanding of underlying biological mechanisms [8]. The Graph Kolmogorov–Arnold Network (GKAN) is a recent advanced GNN model that applies Kolmogorov–Arnold representation theory to graph learning. Unlike conventional GNNs, GKAN enhances interpretability and flexibility by incorporating trainable univariate functions on graph edges [9], [10]. Additionally, the application of spline-based transformations in GKAN enables precise feature extraction and improved transparency suitable for biomarker search in cancer diagnosis tasks.

Gene expression profiles serve as critical research material in cancer science, enabling the monitoring of gene activity in specific tissues and cell populations while distinguishing cancerous cells from healthy ones [11]. Messenger RNA (mRNA) levels indicate actively transcribed genes under specific conditions, providing insights into cancer development and cell progression [12]. Certain genes exhibit elevated or reduced expression in tumors compared to healthy tissues, revealing cellular alterations linked to cancer characteristics [13]. Analyzing gene expression patterns helps identify genes associated with specific cancer types and uncover potential biomarkers for early detection. The integration of gene expression data with DNA methylation and microRNA (miRNA) expression profiles has enhanced cancer biology research [14]. By combining molecular data, researchers can uncover complex interactions across biological levels [15]. DNA methylation analysis sheds light on epigenetic modifications that suppress tumor suppressor genes and activate oncogenes during cancer progression [16]. Similarly, miRNA expression data provides key insights into post-transcriptional gene regulation and its role in tumorigenesis [17]. Integrating gene expression analysis with other omics data has the potential to deepen our understanding of cancer biology and offers new avenues for more effective cancer diagnosis and treatment.

This article introduces the Multi-Omics Graph Kolmogorov–Arnold Network (MOGKAN), a deep learning approach that employs graph-based modeling of mRNA, miRNA, and DNA methylation data for classification of 31 different cancer types. The data preprocessing pipeline involved differential expression analysis (DEG) and Linear Models for Microarray (LIMMA) to select the most informative multi-omics features. DESeq2, which uses a negative binomial model was used for DEG analysis to identify genes with significant expression changes in mRNA data. LIMMA was applied to DNA methylation data to conduct differential analysis, leveraging empirical Bayes methodologies for conducting analyses that decrease standard error uncertainties when computing log-fold changes, thereby increasing detection precision for low-expression genes. The method enables accurate identification of differentially methylated regions (DMRs) with high sensitivity and specificity, making it a valuable tool for epigenetic research and cancer biomarker discovery.

The primary contributions of our work are as follows:

1. Developed a novel approach based on GKAN for cancer classification with inherent feature interpretability through learnable activation functions.
2. Developed a biologically significant graph structure that combines datasets from mRNA, miRNA, and DNA methylation data with the PPI network obtained from the STRING database. The combination of DESeq2 and LIMMA with LASSO allowed for capturing molecular relationships that are crucial for cancer classification.

3. Identified key biomarkers driving cancer progression and validated them using Gene Ontology (GO) and Kyoto Encyclopedia of Genes and Genomes (KEGG) analysis.

The rest of this paper is structured as follows: Section 2 discusses related work on graph-based network architectures and Kolmogorov–Arnold networks. Section 3 describes the datasets, preprocessing pipeline, multi-omics data integration, GKAN architecture, and experimental setup. Section 4 presents the experimental results, analysis, and biomarker discovery. Section 5 lists the limitations of this study and presents future research directions. Finally, Section 6 concludes the paper.

## 2. Related works

The domain of GNNs demonstrates extensive use for understanding structured data representations derived from graph-structure information. Traditional GNN models provide high predictive performance but suffer from two major weaknesses which include reduced interpretability and scalability problems. Researchers have studied Kolmogorov–Arnold Networks (KANs) as an alternative GNN architecture that can address the existing challenges. GKAN unites KANs within graph learning tasks through the adoption of trainable univariate functions in place of conventional linear weights.

Numerous recent works have utilized GKAN for data modeling to improve feature representation and interpretability. Zhang et al. [10] employed GraphKAN by adopting KANs instead of standard activation features to enhance extraction operations. The experimental findings revealed improved effectiveness than standard GNN architectures especially when applied to node and graph classification problems. The framework by Kiamari et al. [9] uses spline-based activation functions between the graph layers to improve performance across different graph structures. The Kolmogorov–Arnold Graph Neural Networks (KAGNNs) by Bresson et al. [18] integrate message-passing techniques derived from KAN to apply the Kolmogorov–Arnold theorem for improved graph learning. KAGNNs demonstrated superior performance than regular GNNs in graph regression tasks, yet showed equivalent results in classification tasks according to their findings. Carlo et al. [19] enhanced the accuracy and interpretability of GKAN through the utilization of spline-based activation functions on edges. Several research projects employed GKAN as a tool for molecular and biomedical applications. Ahmed et al. [20] showed that GKAN can be used in an application that predicts small molecule-protein interaction. The research team of Li et al. [21] developed GNN-SKAN by uniting Swallow-KAN (SKAN) with basic GNNs and obtained leading outcomes throughout multiple molecular data sets.

The growing complexity of biomedical data in multi-omics cancer classification creates an opportunity for GKANs to advance cancer-type predictions as an active research area. GKANs excel at applications requiring transparent explanations because they yield explicit insights into prediction decisions and support variations of input characteristics in personalized medicine and cancer prognostics.

## 3. Materials and Methods

### A. Dataset

Using the GDC query tool from the TCGAbiolinks library [22], the multi-omics data for the various tumors used in this investigation were retrieved from the Pan-Cancer Atlas [23]. The National Cancer Institute launched the Genomic Data Commons project with the goal of providing common databases for cancer genomic studies. The original dataset included 9,171 samples with DNA methylation data, 10,668 samples with mRNA data, and 10,465 samples with miRNA data (Figure 1).

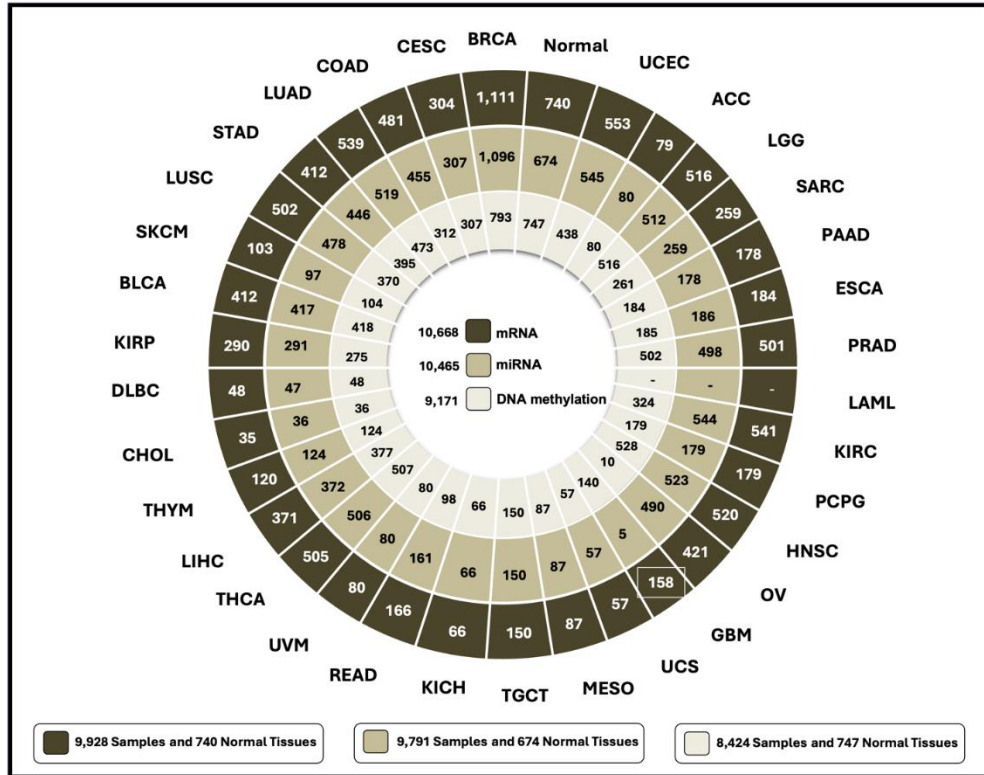


**FIGURE 1.** Tumor types including the number of samples and normal tissues of TCGA Multi-omics data (mRNA, miRNA, and DNA methylation) used in this study.

## B. Data Preprocessing

The data preprocessing pipeline in this study comprises methods for dimensionality reduction to select features in high-dimensional data and methods for finding pertinent biological features in omics data. We employed LIMMA and differential gene expression (DGE) analysis to find the pertinent biological aspects. DESeq2, which uses a negative binomial model to identify genes from mRNA data that have notable changes in the gene expression levels, was specifically used for DGE analysis [22], [24]. To find important differentially methylated CpG sites, LIMMA was applied to DNA methylation data [25]. In order to decrease the dimensionality of the omics data and expand the features selection procedure for mRNA and DNA methylation data, LASSO regression was then used [26]. The following sections outline the phases in the data processing workflow.

### 1. Differential Gene Expression (DGE) Analysis

In genomics, DGE profiling is frequently used to compare the expression levels of genes in a particular organism under various settings or conditions (e.g., normal versus cancer, therapy against control, etc.) [27]. This aids in comprehending the regulation of genes, how their actions are influenced by environmental factors, and a variety of other processes. We used the DESeq2 program to perform differential gene expression on the mRNA data for the current investigation. In order to account for both biological variation and overdispersion, this approach uses a generic linear model of the data count for each gene using a negative binomial distribution. Based on the p-values derived from the Wald statistic, the Wald test was used to determine whether the estimated log fold changes were significant. To determine which genes are likely to be important for the biological processes under study, we set the p-value threshold at 0.001.

## 2. LIMMA

By fitting a linear model for the methylation levels of CpG sites as a function of the experimental sample groups, we used the LIMMA model to carry out differential methylation analysis [28]. The Human Methylation 450K (HM450) array provided 485,577 features and 9,171 samples for the dataset [29]. We identified CpG sites that were substantially methylated in tumors as opposed to normal samples using the LIMMA model. For every CpG site, LIMMA offers a moderated t-statistic along with an effect size estimate that accounts for the relative variations in methylation between the groups. The statistical significance of the differences is indicated by the p-value that matches the t-statistic. After filtering the data using a cutoff p-value of 0.05, there were only 139,321 features left that focused on the most notable methylation alterations.

## 3. LASSO REGRESSION

Lasso Regression functions as a linear regression technique that adds L1 regularization for improving general model performance. The algorithm minimizes squares of residuals along with penalties proportional to absolute coefficient values. The enforcement of this penalty leads to sparsity because it pushes some coefficients to zero, thus removing unimportant features. Lasso Regression is expressed by the following equation:

$$\min_{\beta} \sum_{i=1}^n \left( \gamma_i - \sum_{j=1}^p \chi_{ij} \beta_j \right)^2 + \lambda \sum_{j=1}^p |\beta_j| \quad (1)$$

where  $\gamma_i$  is the observed response variable for the  $i^{\text{th}}$  sample,  $\chi_{ij}$  represents the feature values,  $\beta_j$  are the regression coefficients,  $\lambda$  is the regularization parameter that controls the degree of sparsity is the number of features, and  $n$  is the number of samples. The size of  $\lambda$  parameter determines the level of data regularization, where more coefficients are set to zero when the value is high but fewer features are eliminated at lower  $\lambda$  settings.

**Table 2.** Pipeline for data processing.

Datatype	mRNA	miRNA	DNA Methylation
Original Features	60,660	1881	485,577
Differentially Expressed Analysis (DEGs)	26,768	-	-
LIMMA Model (Selected Features)	-	-	139,321
LASSO Regression Model (Selected Features)	520	-	393
All Tumor Samples and Normal Tissues	10,668	10,465	9,171
Unique Tumor Samples and Normal Tissues	10,667	10,465	8,674
Integrated Data	8,464 Samples and 2,794 Features		

## C. Multi-Omics data integration

Using the sample ID as a key value, we integrated mRNA or RNA-Seq, miRNA, and DNA methylation data for each sample into a single record. Only samples that had all three omics data were kept after applying the inner join merging technique on the sample IDs of the three datasets. Cancer types for which omics data was lacking were excluded from additional analysis. For example, the cancer type "TCGA\_LAML" had no RNA-Seq data, while the cancer type "TCGA\_GBM" had no miRNA data. The final dataset spans 31 cancer types and normal tissues and includes 8,464 samples with 2,794 omics features (Table 2).

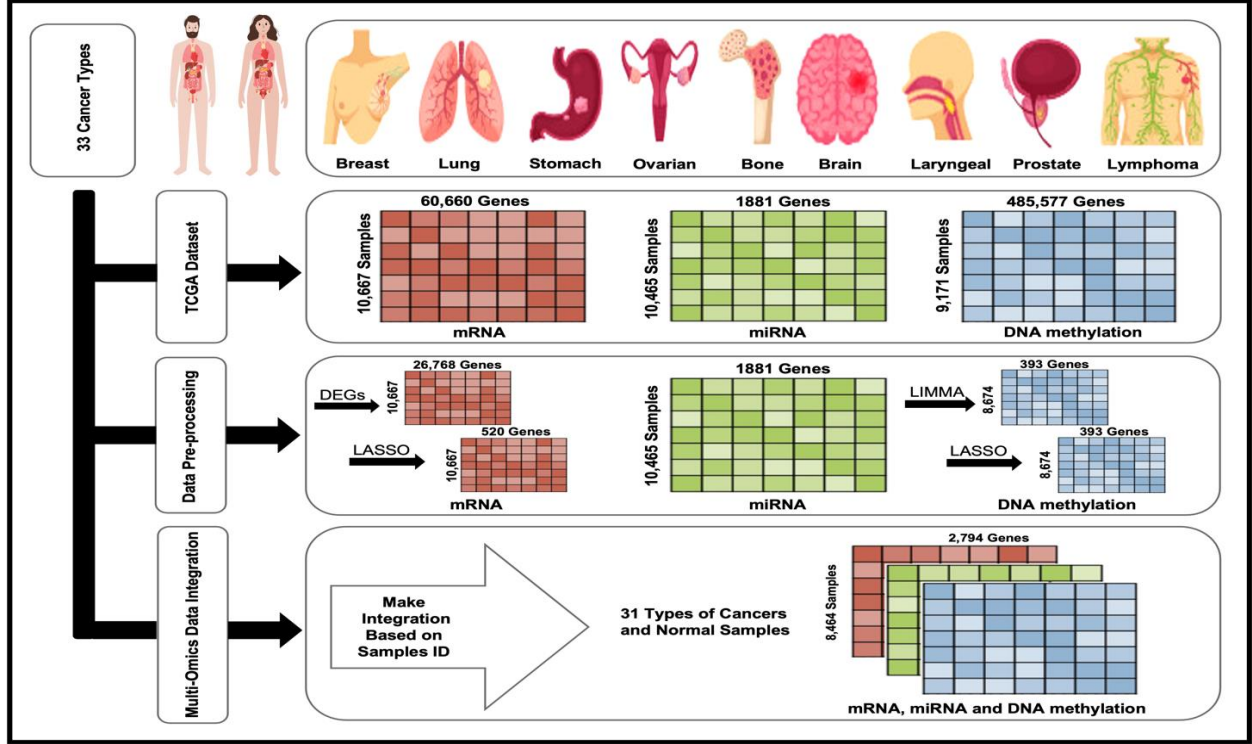


**FIGURE 2.** Preprocessing steps and data integration. Omics data (mRNA, miRNA, and DNA methylation) were obtained from the Pan Cancer Atlas using the TCGAbiolinks library. Next, differential expression analysis (DEG) and LASSO regression were applied to mRNA data, while LIMMA and LASSO regression were applied to DNA methylation data. Subsequently, mRNA or RNA-Seq, miRNA, and DNA methylation data were integrated based on the sample ID using an inner join operation.

## D. Graph Kolmogorov–Arnold Networks (GKAN)

GKAN represents the latest neural architecture which extends the Kolmogorov–Arnold Representation Theorem for graph-structured information along with alternative functionality to Graph Neural Networks via their functional decomposition approach instead of message pass. The decomposition of node and edge interactions into hierarchical learnable transformations in GKANs allows the model to detect long-range dependencies while overcoming the over-smoothing problem that affects deep GNNs. Mathematically they represent a multi-dimensional function through summation expressions of nonlinear one-dimensional functions to derive node embeddings through adaptive transformations procured from neighboring nodes. The Kolmogorov–Arnold theorem states that any continuous multivariate function  $f: \mathbb{R}^d \rightarrow \mathbb{R}$  can be decomposed as:

$$f(x_1, x_2, \dots, x_d) = \sum_{q=1}^{2d+1} g_q \left( \sum_{p=1}^d h_{q,p}(x_p) \right) \quad (2)$$

where  $g_q$  and  $h_{q,p}$  are learnable nonlinear functions,  $x_p$  represents the input features, and  $d$  is the input feature dimension.

For a given graph  $G = (V, E)$ , where  $V$  is the set of nodes and  $E$  is the set of edges, the node features  $h_v^{(l)}$  at a layer  $l$  are updated using:

$$h_v^{(l+1)} = \sum_{q=1}^{2d+1} g_q \left( \sum_{u \in \mathcal{N}(v)} h_{q,p}(h_u^{(l)}) \right) \quad (3)$$

where  $h_v^{(l)}$  is the feature representation of node  $v$  at layer  $l$ ,  $\mathcal{N}(v)$  represents the set of neighboring nodes of  $v$ , and  $g_q$  and  $h_{q,p}$  are trainable transformation functions applied to the graph features. After several layers of hierarchical transformations, the final node representation is obtained as:

$$\hat{y}_v = \sigma \left( \sum_{q=1}^{2d+1} g_q \left( \sum_{p=1}^d h_{q,p}(h_v^{(L)}) \right) \right) \quad (4)$$

where  $\hat{y}_v$  is the predicted class or regression output for node  $v$ ,  $\sigma$  is an activation function such as softmax (for classification) or sigmoid (for binary prediction), and  $L$  is the total number of layers in the network.

## E. Graph structure

The Protein-Protein Interaction (PPI) network demonstrates physical as well as functional protein interactions between proteins to explain cellular procedures and disease pathways. In this study we built the PPI network through the STRING (Search Tool for the Retrieval of Interacting Genes/Proteins) database so that we can access experimental as well as predicted protein interaction data [30]. STRING gathers interactive data from various biological sources including experimental high-throughput results and predicted co-expression events as well as pathway database information with text-mined interactions mined from scientific publications to build its PPI network [31]. The confidence score of each interaction stems from research supporting the connection and infers the reliability of network-building processes [32]. We used the STRING database to extract the relevant subnetwork from proteins corresponding to our study's genes that came from multi-omics data (mRNA, miRNA, and DNA methylation) using the STRING Application Programming Interface (API) version 11.5. This API enables us to obtain Homo sapiens (NCBI taxonomy ID: 9606) specific interaction data for each gene query. The STRING API endpoint retrieved TSV-formatted results with detailed supporting evidence scores that included co-expression, experimental, database, and text-mining data. We used the graph structure as input data for GKAN to create biological relationship models that support classification and biomarker identification procedures.

## F. Experimental setting

Our research experiment tests the classifying capabilities of a Kolmogorov-Arnold Network (KAN) based on multi-omics data. The data includes mRNA and DNA methylation along with miRNA data after performing standardization on the features. A five-fold cross-validation is utilized as it aids in producing stable and broadly applicable predictions. A PPI-based edge index is used for constructing the graph structure by selecting highly interactive proteins from protein-protein interaction networks. This is achieved by determining frequency counts or degrees for all unique proteins. Only proteins that appear at least 200 times in the dataset qualify as highly connected substances according to the defined degree threshold. High-degree proteins are extracted through the filtering process. This process ensures the selection of major hub proteins that stand out in functional and biological networking roles. The KAN model batch normalization together with dropout regularization builds the layers in multiple groups. Hyperparameter optimization was performed via grid search for learning rate, weight decay, number of attention heads, and dropout rate parameters. A training duration of 100 epochs was used to minimize the error loss through the Adam optimizer. The evaluation of performance uses key classification metrics that calculate accuracy, precision, recall, and F1-score per fold prior to averaging the results across all iterations. A feature importance evaluation method identifies the most significant features through the first layer of the trained model. A BioMart query serves to transform the model's top features into their equivalent genes for improved biological meaning. This enables the understanding of

the important biological aspects behind selected features within cancer classification. The pipeline of the proposed approach is depicted in Figure 3.

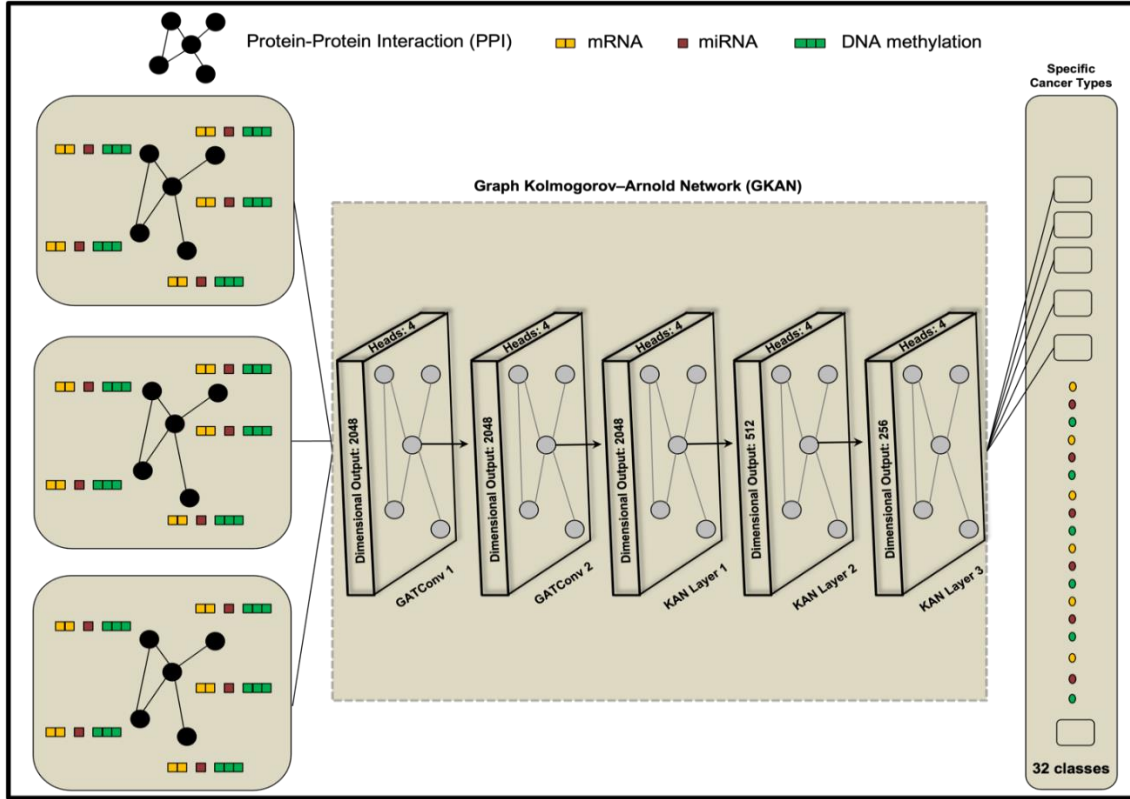


**FIGURE 3.** Architectures of the Multi-Omics Graph Kolmogorov-Arnold Network models for multiclass cancer classification.

## G. Performance measures

We applied standard metrics for multi-class performance evaluation by using accuracy, precision, recall, and F1-score values while extending them with a macro averaging approach for multi-class settings.

The model accuracy serves as a measure of overall correctness which can be defined through the following equation:

$$Accuracy = \frac{\sum_{i=1}^N TP_i}{\sum_{i=1}^N (TP_i + TN_i + FP_i + FN_i)} \quad (5)$$

The averaging methods based on macro-averaging enabled the calculation of precision, recall, and F1-score per class before computing their collective average without preference for any class. The equations of the macro-averaging are as follows:

$$Macro\ Precision = \frac{1}{N} \sum_{i=1}^N \frac{TP_i}{TP_i + FP_i} \quad (6)$$

$$Macro\ Recall = \frac{1}{N} \sum_{i=1}^N \frac{TP_i}{TP_i + FN_i} \quad (7)$$



$$Macro\ F1 - score = \frac{1}{N} \sum_{i=1}^N \frac{2 \times Precision_i \times Recall_i}{Precision_i + Recall_i} \quad (8)$$

## 4. Results and discussion

The performance of our proposed GKAN model which utilizes PPI network as a graph structure is presented in Table 2. Table 2 shows that our model achieves top-level classification results (96.28%  $\pm$  0.0035) for 32 cancer types while processing mRNA, miRNA, and DNA methylation data. The utilization of multi-omics data with GKAN architecture shows a performance boost of 1.58% to 7.30% above the existing methods that utilize Convolutional Neural Network (CNN), Graph Convolutional Neural Network (GCNN), and Graph Transformer Network (GTN) with single-omics methods (Mostavi et al. used 1D-CNN with 95.50% success, Ramirez et al. applied GCNN-PPI with 94.61% success, and Kaczmarek et al. used GTN with an accuracy of 93.56%). KAN architecture in the model ensures reliable protein-protein interaction graph feature extraction because it shows low variability ( $\pm$ 0.0035) which stands out against the instability of hybrid CNNs ( $\pm$ 1.0000).

**TABLE 2.** Performance metrics for related Single-Omics and Multi-Omics graph methods.

Authors & Models	Classes	Multi-Omics Data Type			Accuracy Mean $\pm$ std
		mRNA	miRNA	DNA methylation	
Proposed <b>MOGKAN-PPI graph</b>	32 Classes	√	√	√	<b>96.28 <math>\pm</math> 0.0035</b>
Mostavi et al. [33] <b>1D-CNN</b>		√	-	-	95.50 $\pm$ 0.1000
<b>2D-Vanilla-CNN</b>	34 Classes	√	-	-	94.87 $\pm$ 0.4000
<b>2D-Hybrid-CNN</b>		√	-	-	95.70 $\pm$ 1.0000
Ramirez et al. [34] <b>GCNN-PPI graph</b>	34 Classes	√	-	-	88.98 $\pm$ 0.9000
<b>GCNN-PPI + singleton graph</b>		√	-	-	94.61 $\pm$ 1.0000
Kaczmarek et al. [35] <b>GTN</b>	12 Classes	√	√	-	93.56 $\pm$ 0.9000

The evaluation of the proposed MOGKAN model for cancer type classification is shown in Table 3. We examine single-omics and multi-omics data-set classification results against 31 cancer types and normal tissues using PPI network topology. Among single-omics inputs, mRNA data showed the highest accuracy of 0.9562  $\pm$  0.0029 along with precision values (0.9524  $\pm$  0.0074) and recall (0.9357  $\pm$  0.0094) and F1 score measurements (0.9414  $\pm$  0.0072) which confirms its discriminative classifying capabilities in cancer types. The DNA methylation and miRNA data sets performed closely to the single-omics tests although the results remained slightly below top performance levels. The results demonstrate that the integration of multiple omics modalities enhanced all evaluation metrics performance. The combined use of mRNA with DNA methylation and miRNA resulted in the most effective performance measures including 0.9628  $\pm$  0.0035 accuracy and 0.9582  $\pm$  0.0082 precision together with 0.9445  $\pm$  0.0124 recall and 0.9489  $\pm$  0.0087 F1 score. The MOGKAN framework effectively uses different omics layers' complementary biological signals to produce effective results. These findings emphasize the need for multi-omics integration to improve predictive ability in multi-cancer classification while proving the efficacy of the proposed model for discovering robust biomarkers in an interpretable and data-efficient method.

**Table 3.** Performance metrics of the proposed MOGKAN approach based on PPI Network.

Data Types	Multi-Omics Data Type	Accuracy Mean ± std	Precision Mean ± std	Recall Mean ± std	F1 Score Mean ± std
Single Omics Data	mRNA	<b>0.9562 ± 0.0029</b>	0.9524 ± 0.0074	0.9357 ± 0.0094	0.9414 ± 0.0072
Single Omics Data	miRNA	0.9545 ± 0.0029	0.9497 ± 0.0062	0.9307 ± 0.0091	0.9373 ± 0.0069
Single Omics Data	DNA methylation	0.9551 ± 0.0024	0.9437 ± 0.0121	0.9263 ± 0.0151	0.9324 ± 0.0131
Multi-Omics Data	mRNA and miRNA	0.9553 ± 0.0037	0.9515 ± 0.0087	0.9337 ± 0.0101	0.9396 ± 0.0069
Multi-Omics Data	mRNA and DNA methylation	0.9546 ± 0.0036	0.9519 ± 0.0065	0.9312 ± 0.0091	0.9387 ± 0.0073
Multi-Omics Data	miRNA and DNA methylation	0.9548 ± 0.0047	0.9505 ± 0.0082	0.9319 ± 0.0099	0.9383 ± 0.0084
<b>Multi-Omics Data</b>	<b>mRNA miRNA and DNA methylation</b>	<b>0.9628 ± 0.0035</b>	<b>0.9582 ± 0.0082</b>	<b>0.9445 ± 0.0124</b>	<b>0.9489 ± 0.0087</b>

Table 4 shows the top 10 biomarkers identified by our developed GKAN model based on the importance of the features. The GKAN model selects the biologically relevant features using the calculated weights of these features. Feature importance quantification relies on the computation of absolute weight sums found in the linear transformation layer of the GKAN model. This way the model detects discriminating biomarkers through its weight-based analysis while using BioMart to map significant weight features to known biological entities. The ten biomarkers MCL1, LINC01410, GALNT6, MAML3, ITGB3, LINC01090, PKDCC, PCAT14, KIF16B, and PITPNM3 showed specific functional patterns in different cancer types that matched with established carcinogenesis features. PMID: 28978427 shows that breast cancer patients experienced resistance to therapy because MCL1 functioned as the key regulatory factor that controlled mitochondrial oxidative phosphorylation activity [36]. Additionally (PMID: 39245709) and (PMID: 21481794) show that GALNT6 and PITPNM3 acted as double-function proteins that facilitated both tumor progression through EMT along with immune evasion [37], [38]. The tissue-specific secreted long non-coding RNAs LINC01410 (PMID: 32104067) and LINC01090 (PMID: 34550610) as well as PCAT14 (PMID: 35003397) established integrated ceRNA networks that regulate important pathways and PCAT14 achieved the highest diagnostic precision for prostate cancer (PMID: 35003397) [39], [40], [41]. The research introduced two new extracellular vesicle communication pathways through ITGB3 and KIF16B which demonstrate potential as metastatic CRC biomarkers [PMID: 37040507] and [PMID: 35487942] [42], [43]. (PMID: 37351966) shows that the hypoxia-inducible factor regulates MAML3 activity which subsequently activates both Hedgehog (HH) and NOTCH signaling pathways in gallbladder cancer (GBC). Laboratory research shows MAML3 drives GBC cellular growth together with enhanced cell movement and invasion by initiating NOTCH signaling pathways, but it simultaneously makes tumors more responsive to gemcitabine treatment [44]. (PMID: 35847849) shows that patients with non-small cell lung cancer are affected by PKDCC [45].

**TABLE 4.** Ten high-confidence pan-cancer biomarkers with supporting evidence.

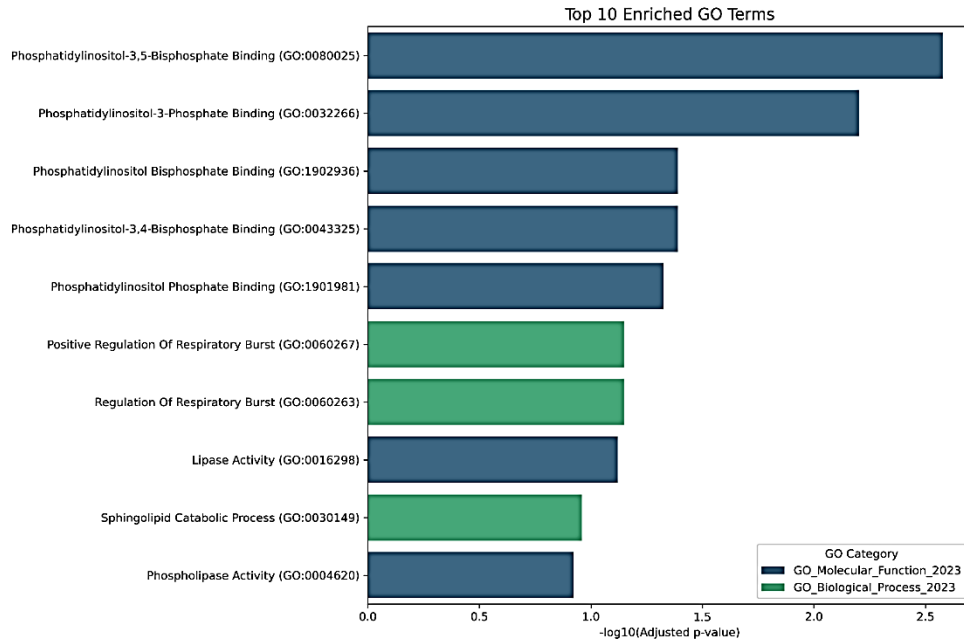
Gene Stable ID	Gene Name	Evidence
ENSG00000143384	MCL1	PMID: 28978427
ENSG00000238113	LINC01410	PMID: 32104067
ENSG00000139629	GALNT6	PMID: 39245709
ENSG00000196782	MAML3	PMID: 37351966
ENSG00000259207	ITGB3	PMID: 37040507

ENSG00000231689	LINC01090	PMID: 34550610
ENSG00000162878	PKDCC	PMID: 35847849
ENSG00000280623	PCAT14	PMID: 35003397
ENSG00000089177	KIF16B	PMID: 35487942
ENSG00000091622	PITPNM3	PMID: 21481794

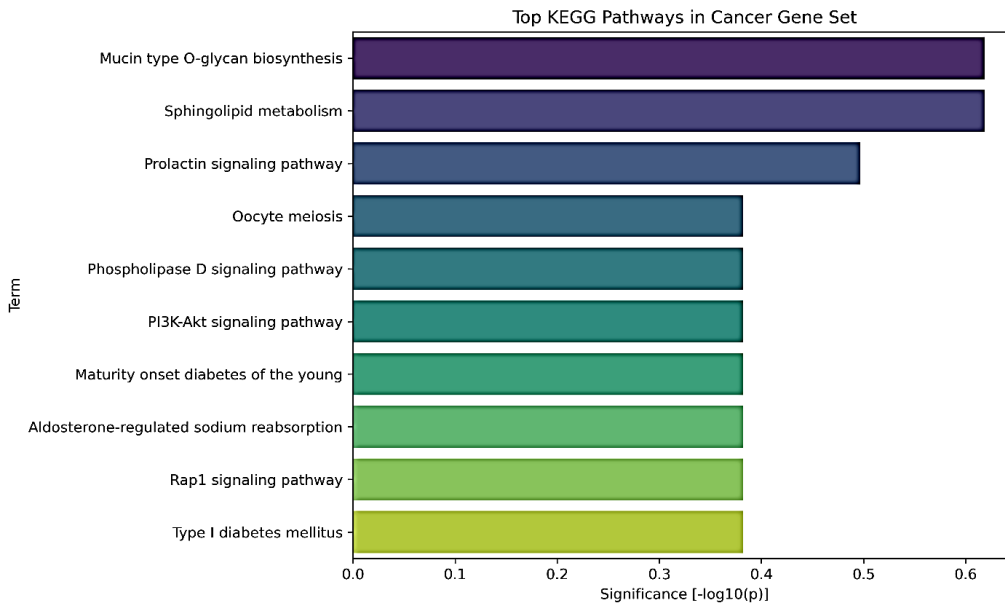
## A. GO and KEGG Analysis

Figure 4 shows that the GKAN analysis generates core GO terms that reveal essential knowledge about molecular systems that drive multi-cancer determination. GKAN effectively identifies fundamental oncogenesis pathways through its strong detection of phosphoinositide binding terms (GO:0080025, GO:0032266). The results from this study confirm existing evidence showing that changes in phosphatidylinositol metabolism are common in cancer types since they activate the PI3K-AKT-mTOR pathway [46] while also contributing to treatment resistance [47]. GKAN successfully identifies biomarkers with pan-cancer use because it specifically detects lipid metabolism functions (GO:0016298 and GO:0004620) which researchers have recognized as fundamental to cancer progression. The identified genes contribute to lipid reprogramming associated with aggressive tumors as per the lipid metabolism terms (GO:0016298 lipase activity and GO:0004620 phospholipase activity) [48]. GKAN demonstrates sensitivity to tumor-immune interactions through its detection of the respiratory burst regulation terms GO:0060267 and GO:0060263 which are essential for multi-cancer classification. The scientific community demonstrated that reactive oxygen species (ROS) dynamics in the tumor microenvironment affect cancer progression and immunotherapy response [49]. The GO term enrichments demonstrate biological validity for the analytical methodology in which GKAN integrates deep learning with multi-omics data representation through graphs. The pathways identified indicate GKAN's successful operation in deriving essential cancer mechanisms from complicated omics datasets.

Figure 5 displays cancer-related gene set enriched KEGG pathways that appear according to their statistical significance values through  $-\log_{10}(p\text{-values})$  ranking. The pathway "Mucin type O-glycan biosynthesis" stands as the most important group because it connects to modifications in tumor cell glycosylation patterns [50]. The Sphingolipid metabolism pathway stands next to "Sphingolipid metabolism" which supports cancer cell survival and drug resistance [51], right after "Sphingolipid metabolism". Following both pathways is "Prolactin signaling pathway" which controls breast cancer progression [52]. Approximately 15% of all cancer-related genes targeted PI3K-Akt signaling pathway which serves as a fundamental regulator between cell proliferation and apoptosis yet remains frequently abnormal in cancer development [46]. The invasive characteristics of the analyzed cancer context become more evident through the involvement of the "Rap1 signaling pathway" which plays a role in cell adhesion and metastasis [53]. The path "Aldosterone-regulated sodium reabsorption" indicates ion transport abnormalities along with disease-specified terms "Type I diabetes mellitus" and "Maturity onset diabetes of the young" which represents shared metabolic changes between cancer and diabetes [54], [55]. The  $-\log_{10}(p)$  values extending to  $\sim 0.6$  demonstrates moderate enrichment while "Mucin type O-glycan biosynthesis" shows the highest degree of enrichment. These data reveal biological pathways that describe mechanisms of cancer development through glycosylation events and lipid transformations and growth factor signaling pathways.



**Figure 4.** Gene ontology enrichment of top 50 multi-cancer biomarkers identified by graph Kolmogorov-Arnold networks.



**Figure 5.** Significantly Enriched KEGG pathways associated with cancer.

## 5. Limitations and Future Works

There are some limitations of the proposed GKAN framework despite its powerful performance and clear explainability. The framework depends on static PPI network information obtained from the STRING database, however, many types of individual cancer-specific protein interactions might be missing. The use of tissue-designated or condition-related interaction networks would improve the biological character of the constructed network. The proposed method uses the multi-omics features mRNA, miRNA, and DNA methylation data, but excluded other features such as proteomics, metabolomics, and copy number variation which could yield supplementary biological insights.

For future work, we intend to include other multi-omics data in our analysis and model construction along with changing interaction networks to boost both model durability and biological understanding capabilities. Also, the use of attention mechanisms for identifying the weight of different omics features can bring improved precision to the prediction outcomes. Extending the model with survival data and treatment responses could convert its identification function into a complete prognostic prediction system. A user-friendly tool combined with a web-based platform for biomedical researchers could be developed to increase accessibility to the GKAN-based methodology in clinical research applications.

## 6. Conclusion

This research introduces MOGKAN, a novel deep learning framework that enables both precise and interpretable cancer classification of multiple types of omics data. Our methodology starts by implementing three successive steps of data preprocessing that combine DESeq2 with LIMMA and LASSO regression to both maintain important biological features and reduce the dimensions of the dataset. MOGKAN achieved outstanding classification performance with 96.28% accuracy in distinguishing 31 cancer types by merging DNA methylation and miRNA and mRNA data with Protein-Protein Interaction networks and exceeded the capabilities of CNNs and GNNs. The model achieves success through its application of Kolmogorov–Arnold theorem which extracts hierarchical features, thus delivering accurate predictions and biological meaning to the results. The model’s identified biomarkers including MCL1, GALNT6, and ITGB3 were verified through GO and KEGG analyses confirming their function in PI3K-AKT signaling and lipid metabolism and immune evasion cancer pathways. The study demonstrates the ability of the proposed method to discover fundamental cancer molecular factors and validates its clinical use in personalized cancer treatment.

## References

- [1] H. Chai, X. Zhou, Z. Zhang, J. Rao, H. Zhao and Y. Yang, "Integrating multi-omics data through deep learning for accurate cancer prognosis prediction," *Computers in biology and medicine*, vol. 134, no. 104481, 2021.
- [2] M. Bersanelli, E. Mosca, D. Remondini, E. Giampieri, C. Sala, G. Castellani and L. Milanese, "Methods for the integration of multi-omics data: mathematical aspects," *BMC bioinformatics*, vol. 17, pp. 167-177, 2016.
- [3] J. L. Ballard, Z. Wang, W. Li, L. Shen and Q. Long, "Deep learning-based approaches for multi-omics data integration and analysis," *BioData Mining*, vol. 17, no. 1, p. 38, 2024.
- [4] G. P. Way and C. S. Greene, "Extracting a biologically relevant latent space from cancer transcriptomes with variational autoencoders," *In PACIFIC SYMPOSIUM on BIOCOMPUTING 2018: Proceedings of the Pacific Symposium*, pp. 80-91, 2018.
- [5] T. N. Kipf and M. Welling, "Semi-supervised classification with graph convolutional networks," *arXiv preprint arXiv*, vol. 1609, no. 02907, 2016.
- [6] W. L. Hamilton, *Graph representation learning*, Morgan & Claypool Publishers, 2020.
- [7] P. Velickovic, G. Cucurull, A. Casanova, A. Romero, P. Lio and Y. Bengio, "Graph attention networks," *stat*, vol. 1050, no. 20, pp. 10-48550, 2018.
- [8] K. Xu, W. Hu, J. Leskovec and S. Jegelka, "How powerful are graph neural networks?," *arXiv preprint*, vol. 1810, no. 00826, 2019.
- [9] M. Kiamari, M. Kiamari and B. Krishnamachari, "GKAN: Graph Kolmogorov-Arnold Networks.," *arXiv preprint*, vol. 2406, no. 06470, 2024.
- [10] F. Zhang and X. Zhang, "GraphKAN: Enhancing Feature Extraction with Graph Kolmogorov Arnold Networks," *arXiv preprint*, vol. 2406, no. 13597, 2024.
- [11] S. Narrandes and W. Xu, "Gene expression detection assay for cancer clinical use," *Journal of Cancer*, vol. 9, no. 13, p. 2249, 2018.

- [12] K. P. Singh, C. Miaskowski, A. A. Dhruva, E. Flowers and K. M. Kober, "Mechanisms and measurement of changes in gene expression," *Biological research for nursing*, vol. 20, no. 4, pp. 369-382, 2018.
- [13] M. Li, Q. Sun and X. Wang, "Transcriptional landscape of human cancers," *Oncotarget*, vol. 8, no. 21, p. 34534, 2017.
- [14] Y. J. Heo, C. Hwa, G. H. Lee, J. M. Park and J. Y. An, "Integrative multi-omics approaches in cancer research: from biological networks to clinical subtypes," *Molecules and cells*, vol. 44, no. 7, pp. 433-443, 2021.
- [15] O. Menyhárt and B. Györfy, "Multi-omics approaches in cancer research with applications in tumor subtyping, prognosis, and diagnosis," *Computational and structural biotechnology journal*, vol. 19, pp. 949-960, 2021.
- [16] F. Geissler, K. Nestic, O. Kondrashova, A. Dobrovic, E. M. Swisher, C. L. Scott and M. J. Wakefield, "The role of aberrant DNA methylation in cancer initiation and clinical impacts," *Therapeutic Advances in Medical Oncology*, vol. 16, no. 17588359231220511, 2024.
- [17] S. J. Ankasha, M. N. Shafiee, N. A. Wahab, R. A. Ali and N. M. Mokhtar, "Post-transcriptional regulation of microRNAs in cancer: From prediction to validation," *Oncology reviews*, vol. 12, no. 1, 2018.
- [18] R. Bresson, G. Nikolentzos, G. Panagopoulos, M. Chatzianastasis, J. Pang and M. Vazirgiannis, "Kagans: Kolmogorov-arnold networks meet graph learning," *arXiv preprint*, vol. 2406, no. 18380, 2024.
- [19] G. D. Carlo, A. Mastropietro and A. Anagnostopoulos, "Kolmogorov-arnold graph neural networks," *arXiv preprint*, vol. 2406, no. 18354, 2024.
- [20] T. Ahmed and M. H. Sifat, "Graphkan: Graph kolmogorov arnold network for small molecule-protein interaction predictions," *In ICML'24 Workshop ML for Life and Material Science: From Theory to Industry Applications*, 2024.
- [21] R. Li, M. Li, W. Liu and H. Chen, "GNN-SKAN: Harnessing the Power of SwallowKAN to Advance Molecular Representation Learning with GNNs," *arXiv preprint*, vol. 2408, no. 01018, 2024.
- [22] A. Colaprico, T. C. Silva, C. Olsen, L. Garofano, C. Cava, D. Garolini, T. S. Sabedot, T. M. Malta, S. M. Pagnotta, I. Castiglioni, M. Ceccarelli, G. Bontempi and H. Noushmehr, "TCGAbiolinks: an R/Bioconductor package for integrative analysis of TCGA data," *Nucleic acids research*, vol. 44, no. 8, pp. e71-e71, 2016.
- [23] J. N. Weinstein, E. A. Collisson, G. B. Mills, K. R. Shaw, B. A. Ozenberger, K. Ellrott and J. M. Stuart, "The cancer genome atlas pan-cancer analysis project," *Nature genetics*, vol. 45, no. 10, pp. 1113-1120, 2013.
- [24] M. D. Robinson, D. J. McCarthy and G. K. Smyth, "edgeR: a Bioconductor package for differential expression analysis of digital gene expression data," *bioinformatics*, vol. 26, no. 1, pp. 139-140, 2010.
- [25] M. E. Ritchie, B. Phipson, D. I. Wu, Y. Hu, C. W. Law, W. Shi and G. K. Smyth, "limma powers differential expression analyses for RNA-sequencing and microarray studies," *Nucleic acids research*, vol. 43, no. 7, pp. e47-e47, 2015.
- [26] R. Tibshirani, "Regression shrinkage and selection via the lasso," *Journal of the Royal Statistical Society Series B: Statistical Methodology*, vol. 58, no. 1, pp. 267-288, 1996.
- [27] F. Rapaport, R. Khanin, Y. Liang, M. Pirun, A. Krek, P. Zumbo, C. E. Mason, N. D. Socci and D. Betel, "Comprehensive evaluation of differential gene expression analysis methods for RNA-seq data," *Genome biology*, vol. 14, pp. 1-13, 2013.
- [28] J. Chen, M. D. Long, S. Sribenja, S. J. Ma, L. Yan, Q. Hu, S. Liu, T. Khoury, C. C. Hong, E. Bandera, A. K. Singh, E. A. Repasky, E. G. Bouchard, M. Higgins, C. B. Ambrosone and S. Yao, "An epigenome-wide analysis of socioeconomic position and tumor DNA methylation in breast cancer patients," *Clinical Epigenetics*, vol. 15, no. 1, p. 68, 2023.
- [29] R. Pidsley, C. C. Wong, M. Volta, K. Lunnon, J. Mill and L. C. Schalkwyk, "A data-driven approach to preprocessing Illumina 450K methylation array data," *BMC genomics*, vol. 14, pp. 1-10, 2013.

- [30] L. J. Jensen, M. Kuhn, M. Stark, S. Chaffron, C. Creevey, J. Muller, T. Doerks, P. Julien, A. Roth, M. Simonovic, P. Bork and C. V. Mering, "STRING 8—a global view on proteins and their functional interactions in 630 organisms.," *Nucleic acids research*, vol. 37, no. (suppl\_1), pp. D412-D416, 2009.
- [31] D. Szklarczyk, A. L. Gable, K. C. Nastou, D. Lyon, R. Kirsch, S. Pyysalo, N. T. Doncheva, M. Legeay, T. Fang, P. Bork, L. J. Jensen and C. V. Mering, "The STRING database in 2021: customizable protein–protein networks, and functional characterization of user-uploaded gene/measurement sets," *Nucleic acids research*, vol. 49, no. D1, pp. D605-D612, 2021.
- [32] A. Franceschini, D. Szklarczyk, S. Frankild, M. Kuhn, M. Simonovic, A. Roth, J. Lin, P. Minguez, P. Bork, C. V. Mering and L. J. Jensen, "STRING v9.1: protein-protein interaction networks, with increased coverage and integration," *Nucleic acids research*, vol. 41, no. D1, pp. D808-D815, 2012.
- [33] M. Mostavi, Y. C. Chiu, Y. Huang and Y. Chen, "Convolutional neural network models for cancer type prediction based on gene expression," *BMC medical genomics*, vol. 13, pp. 1-13, 2020.
- [34] R. Ramirez, Y. C. Chiu, A. Herrera, M. Mostavi, J. Ramirez, Y. Chen, Y. Huang and Y. F. Jin, "Classification of cancer types using graph convolutional neural networks," *Frontiers in physics*, vol. 8, no. 203, 2020.
- [35] E. Kaczmarek, A. Jamzad, T. Imtiaz, J. Nanayakkara, N. Renwick and P. Mousavi, "Multi-omic graph transformers for cancer classification and interpretation," *In Pacific Symposium On Biocomputing 2022*, pp. 373-384, 2021.
- [36] K. M. Lee, J. M. Giltnane, J. M. Balko, L. J. Schwarz, A. L. Guerrero-Zotano, K. E. Hutchinson, M. J. Nixon, M. V. Estrada, V. Sanchez, M. E. Sanders, T. Lee, H. Gomez, A. Lluch, J. A. Perez-Fidalgo, M. M. Wolf, G. Andrejeva, J. C. Rathmell, S. W. Fesik and C. L. Arteaga, "MYC and MCL1 cooperatively promote chemotherapy-resistant breast cancer stem cells via regulation of mitochondrial oxidative phosphorylation," *Cell metabolism*, vol. 26, no. 4, pp. 633-647, 2017.
- [37] X. Sun, H. Wu, L. Tang, A. Al-Danakh, Y. Jian, L. Gong, C. Li, X. Yu, G. Zeng, Q. Chen, D. Yang and S. Wang, "GALNT6 promotes bladder cancer malignancy and immune escape by epithelial-mesenchymal transition and CD8+ T cells," *Cancer Cell International*, vol. 24, no. 1, p. 308, 2024.
- [38] J. Chen, Y. Yao, C. Gong, F. Yu, S. Su, J. Chen, B. Liu, H. Deng, F. Wang, L. Lin, H. Yao, F. Su, K. S. Anderson, Q. Liu, M. E. Ewen, X. Yao and E. Song, "CCL18 from tumor-associated macrophages promotes breast cancer metastasis via PITPNM3," *Cancer cell*, vol. 19, no. 4, pp. 541-555, 2011.
- [39] F. Liu and C. Wen, "LINC01410 knockdown suppresses cervical cancer growth and invasion via targeting miR-2467-3p/VOPP1 axis," *Cancer Management and Research*, pp. 855-861, 2020.
- [40] Y. Chen, X. Zhang, J. Li and M. Zhou, "Immune-related eight-lncRNA signature for improving prognosis prediction of lung adenocarcinoma," *Journal of clinical laboratory analysis*, vol. 35, no. 11, p. e24018, 2021.
- [41] Y. Yan, J. Liu, Z. Xu, M. Ye and J. Li, "lncRNA PCAT14 is a diagnostic marker for prostate cancer and is associated with immune cell infiltration," *Disease Markers*, vol. 2021, no. 1, p. 9494619, 2021.
- [42] W. Guo, Y. Cai, X. Liu, Y. Ji, C. Zhang, L. Wang, W. Liao, Y. Liu, N. Cui, J. Xiang, Z. Li, D. Wu and J. Li, "Single-exosome profiling identifies ITGB3+ and ITGAM+ exosome subpopulations as promising early diagnostic biomarkers and therapeutic targets for colorectal cancer," *Research*, vol. 6, no. 0041, 2023.
- [43] Q. Zhao, F. Wang, Y. X. Chen, S. Chen, Y. C. Yao, Z. L. Zeng, T. J. Jiang, Y. N. Wang, C. Y. Wu, Y. Jing, Y. S. Huang, J. Zhang, Z. X. Wang, M. M. He, H. Y. Pu, Z. J. Mai, Q. N. Wu, R. Long, X. Zhang, T. Huang, M. Xu, M. Z. Qiu, H. Y. Luo, Y. H. Li, D. S. Zhang and W. H. Jia, "Comprehensive profiling of 1015 patients' exomes reveals genomic-clinical associations in colorectal cancer," *Nature communications*, vol. 13, no. 1, p. 2342, 2022.
- [44] L. NA, H. ONISHI, S. MORISAKI, S. ICHIMIYA, Y. YAMADA, S. MASUDA, S. NAGAO, S. KOGA, K. NAKAYAMA, R. IMAIZUMI, Y. ODA and M. NAKAMURA, "MAML3 Contributes to Induction of Malignant Phenotype of Gallbladder Cancer Through Morphogenesis Signalling Under Hypoxia," *Anticancer research*, vol. 43, no. 7, pp. 2909-2922, 2023.

- [45] J. Du, B. Wang, M. Li, C. Wang, T. Ma and J. Shan, "A novel intergenic gene between SLC8A1 and PKDCC-ALK fusion responds to ALK TKI WX-0593 in lung adenocarcinoma: a case report," *Frontiers in Oncology*, vol. 12, no. 898954, 2022.
- [46] D. A. Fruman, H. Chiu, B. D. Hopkins, S. Bagrodia, L. C. Cantley and R. T. Abraham, "The PI3K pathway in human disease," *Cell*, vol. 170, no. 4, pp. 605-635, 2017.
- [47] G. Hoxhaj and B. D. Manning, "The PI3K–AKT network at the interface of oncogenic signalling and cancer metabolism," *Nature Reviews Cancer*, vol. 20, no. 2, pp. 74-88, 2020.
- [48] L. A. Broadfield, A. A. Pane, A. Talebi, J. V. Swinnen and S. M. Fendt, "Lipid metabolism in cancer: New perspectives and emerging mechanisms," *Developmental cell*, vol. 56, no. 10, pp. 1363-1393, 2021.
- [49] H. Sies, V. V. Belousov, N. S. Chandel, M. J. Davies, D. P. Jones, G. E. Mann, M. P. Murphy, M. Yamamoto and C. Winterbourn, "Defining roles of specific reactive oxygen species (ROS) in cell biology and physiology," *Nature reviews Molecular cell biology*, vol. 23, no. 7, pp. 499-515, 2022.
- [50] I. Brockhausen, "Mucin-type O-glycans in human colon and breast cancer: glycodynamics and functions," *EMBO reports*, vol. 7, no. 6, pp. 599-604, 2006.
- [51] Y. A. Hannun and L. M. Obeid, "Sphingolipids and their metabolism in physiology and disease," *Nature reviews Molecular cell biology*, vol. 19, no. 3, pp. 175-191, 2018.
- [52] V. Goffin, N. Binart, P. Touraine and P. A. Kelly, "Prolactin: the new biology of an old hormone," *Annual review of physiology*, vol. 64, no. 1, pp. 47-67, 2002.
- [53] M. Gloerich and J. L. Bos, "Regulating Rap small G-proteins in time and space," *Trends in cell biology*, vol. 21, no. 10, pp. 615-623, 2011.
- [54] A. Spat and L. Hunyady, "Control of aldosterone secretion: a model for convergence in cellular signaling pathways," *Physiological reviews*, vol. 84, no. 2, pp. 489-539, 2004.
- [55] E. J. Gallagher and D. LeRoith, "Obesity and diabetes: the increased risk of cancer and cancer-related mortality," *Physiological reviews*, vol. 95, no. 3, pp. 727-748, 2015.